Beam Measurements on a Small Commercial Cyclotron

R.E. Laxdal, A. Altman, T. Kuo
TRIUMF, 4004 Wesbrook Mall, Vancouver, B.C., Canada V6T 2A3
T. Kadantsev
JINR, Dubna, Russia

Abstract

A 13 MeV H^- cyclotron for PET isotope production, the TR13, has been designed and built at TRIUMF in collaboration with a commercial partner. As part of the commissioning and documentation procedure the fundamental beam parameters at extraction have been measured including the transverse circulating emittance, the spot size on target, the radial centering error, and the energy spread in the extracted beam. The simple, yet effective, measurement set-up and data acquisition system will be described and the results presented.

1 INTRODUCTION

The TR13 [1] (Fig. 1) is a 13 MeV cyclotron with a magnet capable of 18 MeV and a peak beam intensity of 100 μA. The cyclotron is capable of simultaneous extraction to two self-shielded semi-automatic targets. The magnet has four sectors with two rf resonators in opposite valleys operating at 73 MHz the fourth harmonic of the orbit frequency. The rf voltage is 50 kV yielding a peak energy gain per turn of 200 keV. An H^- CUSP source operates external to the cyclotron and injection is axial through a spiral inflector. [2] The magnet design [3] was completed by May 1992, the magnet shimming [4] by May 1993, and the initial 1 MeV beam test [2] was completed by August 1993.

Turns merge during acceleration as the large phase band ($\sim \pm 20°$) generates energy spread. The radius gain per turn, dR/dn, at extraction (3.3 mm) is of the same order as the expected incoherent amplitude (2.2 mm for $\epsilon_x = 2\pi\mu$m) and so a uniform radial density exists, and extraction occurs over multiple turns.

2 MEASURING TECHNIQUES

The measurement methods are standard (see for example [5]) and were chosen to minimize cost and, where possible, to utilize existing equipment.

2.1 Axial Emittance

The circulating axial emittance can be indirectly determined by measuring the beam half height, $z_{\frac{1}{2}}$, by scanning a probe axially. The probe head must be wide compared to the radial extent of one axial precession cycle, and the beam centered and the median plane flat compared to the incoherent amplitude. The relation $z_{\frac{1}{2}} = \sqrt{\epsilon_z \beta_z}$ can be used to calculate the emittance.

2.2 Radial Emittance

An estimate of the horizontal emittance can be found by using a stationary totally intercepting post at the energy of interest and a radially scanning probe. A scan is made with the probe at the same azimuth as the blocker and repeated with the probe (or, if not possible, the blocker) 180° downstream. The radial width of the shadow region π downstream from the blocker will extend from $R_{block} - 2x_{\frac{1}{2}}$ to $R_{block} + 2x_{\frac{1}{2}}$ where $x_{\frac{1}{2}}$ is the radial half width from incoherent oscillations. For this to be true the radial tune, ν_r, must be close to 1 and the centering error, A_c, must be less than both the incoherent betatron amplitude, A_i, and the radius gain per turn, dR/dn, so that $A_c \cdot \sin 2\pi(\nu_r - 1)$ is much less than both A_i and dR/dn. The radial range over which the recorded intensity on a totally intercepting probe 'falls-off' will be the spot size on the probe, $\sim dR/dn$, at the azimuth of the blocker and $dR/dn + 4x_{\frac{1}{2}}$ 180° downstream. By comparing the two scans we can solve for the half width and use $x_{\frac{1}{2}} = \sqrt{\epsilon_x \beta_x}$ to calculate the radial emittance.

A simple simulation code [7] was written to help predict the shape of the 'fall-off' curves for various initial emittances. The initial radial beam distribution is Gaussian. The curves can be compared with actual 'fall-off' curves to help determine the radial emittance, the centering error and the distribution of beam in radial phase space compared to a Gaussian.

2.3 Radial Centering Error at Extraction

The radial centering error can be found by utilizing the post and probe set-up explained above. By varying the rf frequency, the number of turns to the outside, hence the phase of the centering error, is altered and the position of the shadow region π downstream from the post will shift. For ν_r =1.06 the phase advance at extraction is $2\pi(\nu_r - 1)$=0.12π/turn hence the addition of 5–10 turns is enough to significantly change the phase of the centering error. The number of turns, N, required to reach a certain energy, E_f, while detuning the frequency by Δf satisfies $E_f/(hV_d)$ =sin$(kN)/k$ where $k = 2\pi h \frac{\Delta f}{f}$, V_d is the dee voltage, and h is the rf harmonic. Assuming perfect isochro-

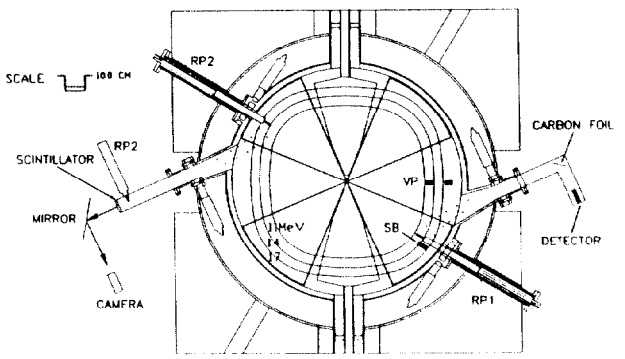

Figure 1: The TR13 cyclotron shown from the side (vertical midplane). Shown are the two radial probes, RP1 and RP2, the stationary blocker at 13 MeV, SB, and the two axial probe head positions at 11 and 17 MeV, VP. Other measuring equipment is shown at the two target stations. Only the target station on the left was actually utilized.

nism, a change of 30 kHz is needed to increase the number of turns by 6 from 65 to 71 at 13 MeV.

2.4 Isochronism

A rough estimate of the isochronism and the accelerated phase band can be deduced from the response of beam transmission to rf frequency variation [5]. Loss occurs when $\sin\phi_m + \sin\phi_b + \Delta\sin\phi_f = \pm 1$, where ϕ_b is the half width of the longitudinal phase band, and ϕ_f and ϕ_m are the phase shifts due to the frequency swing and to isochronism errors in the magnet respectively. The range of $\Delta\sin\phi_f$ values over which loss occurs corresponds to the longitudinal bunch length. The width of the lossless plateau can be used to roughly determine the limits of the phase wander near the radii of interest. The uncertainty in the method lies in not knowing exactly at what radius the loss takes place unless data is taken at a large number of radii. However, since the phase slip increases with radius and the magnet survey predicts good isochronism, loss would normally occur near the monitoring probe.

2.5 Extracted Energy Spread

Elastic scattered protons from a carbon foil can be energy analyzed in a solid state silicon detector connected to a multichannel analyzer. The energy spread in the extracted beam can be calibrated by comparing the width of the elastic peak with the position of the peak from the first excited state 4.4 MeV away. The flux of scattered particles can be controlled by altering the scattering angle.

2.6 Spot Size on Target

Two complimentary measurement methods were used. In the first a graduated scintillator was placed at the target location and the beam size viewed via TV camera. In this way parameters such as rf frequency, foil location, and source and injection line settings could be altered and the effects observed in real time. Tail formation due to non-linear behaviour is easily observed. The second method involves positioning a probe that can sweep separately through the axial and the dispersive planes to measure the beam profile on target. The response is more linear than with the scintillator and the results offer an independent assessment of the transverse emittance.

3 DIAGNOSTICS AND CONTROLS

Fig. 1 gives a summary of the experimental set-up. Two water cooled totally intercepting probes are used for all scanning measurements. For radial measurements the probes (RP1 and RP2) span the energy range from 11–19 MeV. For axial tests RP1 was removed, refitted with a new head, VP and driven axially through a pump port in the valley floor. The head is attached to an L-arm extending from the probe axis and can be positioned to contact the beam in two radial positions along the center of the valley, at energies of 11 and 17.5 MeV.

The data acquisition process used standard TRIUMF equipment. A CAMAC crate sits on the serial highway with motor controls, signal amplifiers and ADC readbacks. Two TRIMAC[1] motor control channels provide for remote control and monitoring of the probes. The raw current signals are fed to a CAMAC 6-range amplifier and in turn to a 14-bit ADC. The digital signal is read by the computer and written to file. A set of routines were implemented on an X-window terminal using a Motif based user interface and the PLOTDATA graphical package.

[1]TRIUMF CAMAC Auxiliary Crate Controller

4 TEST RESULTS

4.1 Radial Emittance and Centering Error

The radius gain per turn at 13 MeV was measured with RP1 to be 3.2 mm. The radial width of the fall-off region π downstream from the blocker measured with RP2 varies with cyclotron setting but is roughly 11 mm, giving an incoherent amplitude of $\sim$2 mm and a radial emittance of $\sim 1\pi\mu$m. The centering error is less than 1 mm.

A more accurate estimate of emittance and the centering error is found by fitting the radial scans to the calculated scans at various rf frequencies. Both the initial radial width in the calculation and the position of the predicted curve were altered to establish a fit. The comparisons show that the beam is not perfectly Gaussian but rather has a bright core of amplitude $\sim$2 mm accompanied with long tails. Also the distribution changes with rf frequency. This is representative of a case where either a mis-matched stretched beam exists or a group of extreme phases are radially off center. The results of the fit for 13 MeV are shown in Fig. 2. The position is given with respect to some arbitrary reference and corresponds to a 0.6 mm centering error. The beam half width, for 90% of the beam, varies as the assumed mismatched beam precesses. The average is $\sim$2 mm, corresponding to a radial emittance of $1.3\pi\mu$m.

4.2 Axial Measurements

Cyclotron optimization reduced the measured axial emittance to $\sim 3.5\pi\mu$m for 90% of the beam. A sample analysis of an axial scan at 11 MeV is shown in Fig. 3. Measurements were taken at a number of different settings of the injection system. For some scans a more rounded, larger emittance was measured, evidence of a somewhat hollow beam. This is caused by the beam being injected off-center and experiencing decoherence during acceleration. The axial emittance was dependent on the beam intensity. For beam intensities of 0.7 μA, 2.5 μA, and 7.5 μA the emittances were 3.5π, 3.3π and 3.1π respectively. This agrees with earlier tests which showed that source emittance improved as output intensities increased up to 1 mA.

4.3 Isochronism and Phase Band

After removing the copper blocker at 13 MeV the beam transmission to both 13 MeV and 18 MeV were monitored as func-

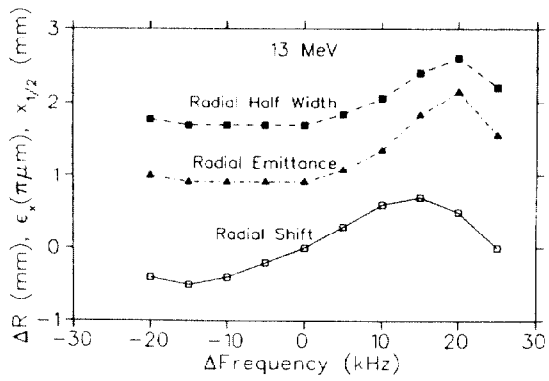

Figure 2: Results of fitting calculated fall-off curves to experimental scans at different rf frequencies. Both the beam width for 90% of the beam enclosed and the position of the calculated curves were varied. The radial emittance is calculated from the width.

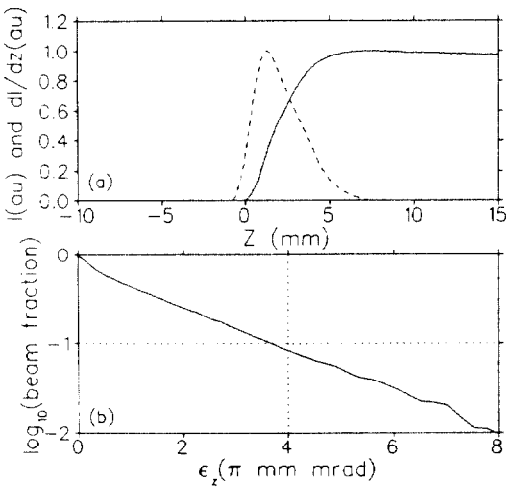

Figure 3: Measured axial half-width of the beam from a axial probe scan at 11 MeV and corresponding fraction of the beam lying outside a given emittance.

tions of rf frequency. The results are plotted in Fig. 4 as a function of $\Delta\sin\phi$. When the curves are differentiated the fall-off region corresponds to $2\Delta\sin\phi_b$=0.6 at FWHM and 1.0 at 10% of the maximum. The longitudinal distribution looks Gaussian in nature. The phase wander due to non-isochronism, spans the range $\sin\phi_m$=−0.16 - 0.25 for 13 MeV and $\sin\phi_m$=−0.17 - 0.34 for 18 MeV. This can be compared with the calculated phase wander based on the magnet survey field where the variation in the outer region is no more than ±5° [8] which is slightly smaller than the measured values listed above.

4.4 *Beam Spot on Target*

Beam is extracted by fitting RP2 with a foil. A short beampipe is attached at the target location with axial and azimuthal side ports. RP1 is moved from the cyclotron to either port to measure the beam distribution in both the dispersive and axial planes (Fig. 1). Just downstream of this position a scintillator is placed and a TV camera with a video framegrabber is used to record visual images of the beam spot. The spot is roughly circular with a diameter of 10 mm. Although the population in the tails changes somewhat with frequency and

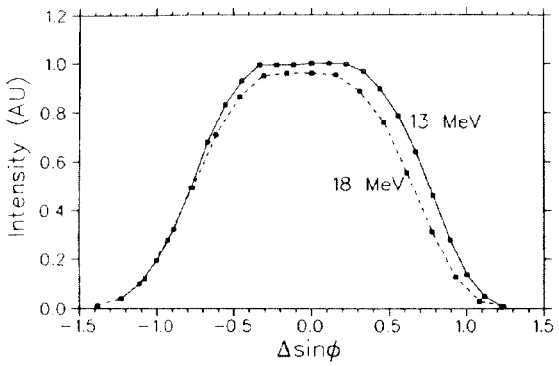

Figure 4: The beam transmission to 13 MeV and 18 MeV as a function of rf frequency here converted to $\Delta\sin\phi$.

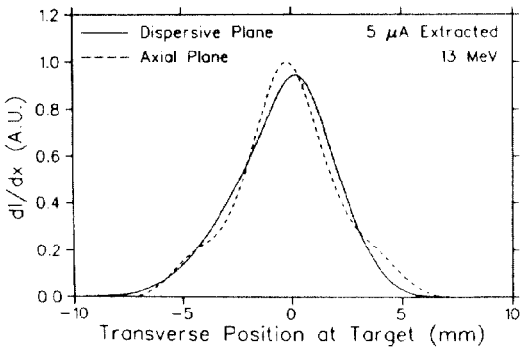

Figure 5: Distribution of beam on target in dispersive and non-dispersive planes.

injection line settings the core remains the same.

The beam intensity distributions on the target for 13 MeV are shown in Fig. 5 for both the dispersive and non-dispersive planes. 90% of the beam is within a spot size of 8 mm×8 mm. This agrees well with ray-tracing calculations [9] based on transverse emittances of $(\epsilon_x, \epsilon_z) = (1.3\pi, 3.5\pi)\mu$m.

4.5 *Energy Spread*

A schematic of the equipment set-up for the energy spread measurement is shown in Fig. 1. A carbon foil is placed in the target chamber at 45° to the incident beam. A beam pipe section is attached to the target chamber at 90° to the beam direction and a silicon detector is placed in the pipe ∼1 m from the foil. The measured energy spread for 90% of the beam was ∼380 keV. The detector resolution (20 keV) and kinematic broadening (40 keV) contributed only ∼1% to the width. Based on the measured radial emittance of $1.3\pi\mu$m the expected energy spread for 90% of the beam is ΔE=430 keV. Beam intensities of from 200 nA to 2 μA were measured. Above these values detector saturation was apparent.

5 REFERENCES

[1] M. Dehnel, *et al.* Proc. of the European Part. Acc. Conf., Berlin 1992, p. 1682.

[2] T. Kuo, *et al.*, *Performance of an ISIS System using Compact Magnetic Quadrupoles*, these proceedings.

[3] L. Root, R.E. Laxdal, A. Papash, *TR13 Magnet Design*, TRIUMF Design Note, TRI-DN-93-14, May 1993.

[4] W. Giles, private communication

[5] A.A. Garren and L. Smith, *Diagnosis and Correction of Beam Behaviour in an Isochronous Cyclotron*, CERN 63-19 (1963), p. 18.

[6] R.E. Laxdal, *et al.*, Proc. of the 13th Intl. Conf. on Cyc. and their Applic., Vancouver, 1992, p. 415.

[7] R.E. Laxdal, *et al.*, *Beam Quality Tests on the TR13 Cyclotron*, TRIUMF Design Note, to be issued.

[8] L. Root, private communication.

[9] R.E. Laxdal, *Final Extraction Calculations for the TR13 Cyclotron*, TRIUMF Design Note, to be issued.